



# A physically motivated parametric model for compact representation of room impulse responses based on orthonormal basis functions

Giacomo Vairetti, Enzo De Sena, Toon van Waterschoot\*, Marc Moonen  
Dept. of Electrical Engineering (ESAT), STADIUS Center for Dynamical Systems, Signal Processing and Data Analytics, KU Leuven, Kasteelpark Arenberg 10, 3001 Leuven, Belgium.

Michael Catrysse  
Televic N.V., Leo Bekaertlaan 1, 8870 Izegem, Belgium.

Neofytos Kaplanis†  
Bang & Olufsen A/S, Peter Bangs Vej 15, 7600 Struer, Denmark.

Søren Holdt Jensen  
Dept. of Electronic Systems, Aalborg University, Niels Jernes Vej 12, 9220 Aalborg, Denmark.

## Summary

A Room Impulse Response (RIR) shows a complex time-frequency structure, due to the presence of sound reflections and room resonances at low frequencies. Many acoustic signal enhancement applications, such as acoustic feedback cancellation, dereverberation and room equalization, require simple yet accurate models to represent a RIR. Parametric modeling of room acoustics attempts at approximating the Room Transfer Function (RTF), for given positions of source and receiver inside a room, by means of rational functions in the  $z$ -domain that can be implemented through digital filters. However, conventional parametric models, such as all-zero and pole-zero models, have some limitations. In this paper, a particular fixed-pole Infinite Impulse Response (IIR) filter based on Orthonormal Basis Functions (OBFs) is used as an alternative, motivated by its analogy to the physical definition of the RIR as a Green's function of the acoustic wave equation. An accurate estimation of the model parameters allows arbitrary allocation of the spectral resolution, so that the room resonances can be described well and a compact representation of a target RIR can be achieved. The model parameters can be estimated by a scalable matching pursuit algorithm called OBF-MP, which selects the most prominent resonance at each iteration. A modified version of the algorithm, called OBF-GMP (Group Matching Pursuit), is introduced for the estimation of a common set of poles from multiple RIRs measured at different positions inside a room. A new database of RIRs measured in a rectangular room using a subwoofer is also presented. Simulation results using this database show that, in comparison to OBF-MP, the OBF-GMP significantly reduces the number of parameters necessary to represent the RIRs.

PACS no. xx.xx.Nn, xx.xx.Nn

## 1. Introduction

A Room Impulse Response (RIR) shows a complex time-frequency structure, due to the presence of room resonances at low frequencies and the intricate tempo-

ral structure of sound reflections. Parametric models are used in all those acoustic signal enhancement applications that require the RIR to be represented in a simple yet accurate way. Examples of these applications are acoustic feedback cancellation, dereverberation, and room equalization. In parametric modeling, a Room Transfer Function (RTF), corresponding to a Green's function of the acoustic wave equation for specific positions of the loudspeaker and the microphone inside a room, is represented by means of a rational function in the  $z$ -domain and implemented through digital filters. This rational function can be written in

---

(c) European Acoustics Association

\* also affiliated with the Dept. of Electrical Engineering (ESAT-ETC), AdvISE Lab, KU Leuven, Kleinhoefstraat 4, 2440 Geel, Belgium.

† also affiliated with the Dept. of Electronic Systems, Aalborg University, Niels Jernes Vej 12, 9220 Aalborg, Denmark.

terms of zeros and poles by computing the complex-valued roots of the numerator and denominator polynomials, respectively. However, conventional parametric models, such as all-zero and pole-zero models, present some limitations. The *all-zero* model [1] uses a Finite Impulse Response (FIR) filter to approximate the sampled RIR, with the number of parameters corresponding to the sample index at which the RIR is truncated. A zero approximation error is obtained up to the truncation index, but a large number of parameters is required in order to capture the resonant characteristics of the room, especially when the reverberation time is high. Moreover, the parameter values are strongly dependent on the source and receiver positions. *All-pole* and *pole-zero* models are used in an attempt to overcome these limitations. These models use pairs of complex-conjugate poles to represent resonances in the RTF. This enables to reduce the number of parameters and to obtain parameter values less sensitive to changes in the source and receiver positions. However, a stable all-pole model cannot represent true delays nor the non-minimum-phase characteristics of the RTF [1]. Pole-zero models [2], on the other hand, represent resonances and damping constants by the poles of the RTF, and anti-resonances and time delays by its zeros. The *Common-Acoustical-Pole and Zero* (CAPZ) model [3] exploits the fact that room resonances are independent of the position of the source and receiver, but are rather a characteristic of the room itself. As the name suggests, the RTFs measured at different positions in the room are parametrized by a common set of poles, while differences between these responses are described by different sets of zeros. In this way, a more compact representation of a group of RIRs is obtained. However, since the poles appear nonlinearly in the pole-zero model, no closed-form solution to the parameter estimation problem exists, thus requiring nonlinear optimization techniques, possibly leading to instability or convergence to local minima.

An alternative to conventional parametric models is provided by a particular family of models based on orthonormal basis functions. *Orthonormal Basis Function* (OBF) models [4, 5, 6] define a fixed-pole IIR filter, which is an orthonormalized parallel connection of second-order resonators, whose impulse responses represent damped sinusoids. Then, the RIR approximation is built as a linear superposition of a finite number of exponentially decaying sinusoids, whose frequency and decay rate is determined by the position of the poles inside the unit circle. The analogy with the definition of the RTF is clear. Each term of the Green's function corresponds to a resonator whose impulse response is a sinusoid, oscillating at a particular resonance frequency and damped with a particular damping constant [7]. OBF models possess many other desirable properties, such as orthogonality and stability. These models are also very flexible, in

the sense that poles can be distributed arbitrarily inside the unit circle of the  $z$ -plane, thus giving freedom in the allocation of the spectral resolution. However, since OBF models are nonlinear in the pole parameters, estimating the poles that provide a good approximation of a given RIR is a nonlinear problem. Nonlinear optimization techniques have been proposed for the optimization of the poles in different applications, such as acoustic echo cancellation [8] and loudspeaker and room modeling [9]. In [10], the nonlinear problem was avoided by iteratively selecting poles from a discrete grid using a scalable matching pursuit algorithm, called OBF-MP.

This paper introduces a modified version of the OBF-MP that aims at estimating a set of poles common to multiple RIRs measured at different positions in the same room. It is shown that the modified algorithm, termed here OBF-GMP, approximates the set of RIRs more accurately, compared to the case when the poles are estimated individually for each RIR or when the all-zero model is used, with the same total number of parameters. Simulations have been performed on a database of RIRs measured at different positions inside a rectangular room, with a subwoofer source.

The paper is structured as follows. OBF models are described in Section 2. In Section 3, the OBF-GMP algorithm is introduced. Section 4 describes the RIR database measurements. Simulation results are presented in Section 5. Section 6 concludes the paper and indicates possible directions for future work.

## 2. OBF models

OBF models define an IIR filter structure that allows to incorporate information about the resonant and damping behavior of a system. Although these models are widely used in system identification and control applications, only a few examples of their use in room acoustics modeling are known [8, 9, 10, 11]. Under fairly realistic assumptions, a room can be considered as a causal, stable, and linear system, which is characterized by a number of room resonances, or modes. A mode is represented in the  $z$ -domain by a second-order resonator defined by a pair of complex-conjugate poles  $\{p_i, p_i^*\}$ , with transfer function

$$P_i(z) = \frac{1}{(1 - p_i z^{-1})(1 - p_i^* z^{-1})} \quad (1)$$

with  $*$  indicating complex conjugation. The impulse response corresponding to the transfer function in (1) is an exponentially decaying sinusoid, sampled at frequency  $f_s$ , oscillating at the resonant frequency  $\omega_i$  and decaying exponentially accordingly to the damping constant  $\zeta_i$ , which also determines the bandwidth of the resonance. Thus, the angle  $\vartheta_i = \omega_i/f_s$  and the radius  $\rho_i = e^{-\zeta_i/f_s}$  of the pole pair  $\{p_i, p_i^*\} = \rho_i e^{\pm j\vartheta_i}$

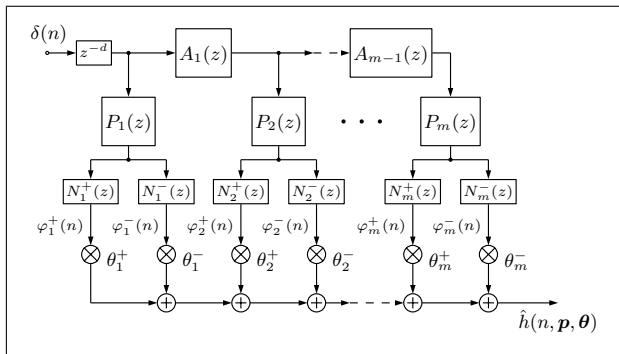


Figure 1. The generalized OBF model structure for  $m$  pairs of complex-conjugate poles.

determine the shape of the resonance. For instance, poles close to the unit circle correspond to room modes with long decay time and high Q-value. Multiple resonances can be represented by a parallel connection of second-order resonators. The resulting filter structure, also called parallel second-order filter [12], originates from a partial fraction expansion of the pole-zero RTF. The terms corresponding to a pair of complex-conjugate poles  $\{p_i, p_i^*\}$  are combined to form a second-order IIR filter with real-valued coefficients and transfer function as in (1), which produces a pair of real-valued responses, one being the one-sample delayed version of the other. The output of this filter structure is then a linear combination of pairs of damped sinusoids, which are used as basis functions in a linear-in-the-parameters model.

OBF models originate from the orthonormalization of the parallel second-order filter, where orthogonality between any two consecutive basis functions is enforced by a second-order all-pass filter,

$$A_i(z) = \frac{(z^{-1} - p_i)(z^{-1} - p_i^*)}{(1 - p_i z^{-1})(1 - p_i^* z^{-1})}, \quad (2)$$

in which the zeros in  $1/p_i$  and  $1/p_i^*$  ensure that the basis functions defined by  $\{p_{i+1}, p_{i+1}^*\}$  are orthogonal to those generated by  $\{p_i, p_i^*\}$ . The two basis functions of each pole pair are normalized and made orthogonal to each other by a pair of orthonormalization filters  $N_i^\pm(z)$ . The general filter structure of an OBF model is shown in Figure 1 for  $m$  pairs of complex-conjugate poles. Different choices are available for the orthonormalization filters, as explained in [6]. In this work, the so-called Kautz model [13] is used, where

$$N_i^\pm(z) = |1 \pm p_i| \sqrt{\frac{1 - |p_i|^2}{2}} (z^{-1} \mp 1). \quad (3)$$

OBF models present many interesting properties. Firstly, as opposed to pole-zero models, poles can be positioned anywhere inside the unit circle without problems of numerical ill-conditioning. This also allows to allocate a higher spectral resolution in the frequency range of interest.

Secondly, the OBFs form a complete set in the Hardy space on the unit disc under the mild assumption that  $\sum_{i=1}^{\infty} (1 - |p_i|) = \infty$  [6]. Thus, any stable linear filter can be approximated with arbitrary accuracy by a linear combination of a certain finite number of OBFs, so that OBF models can achieve an accurate approximation of a RIR with a reduced number of parameters, compared to conventional models.

A third important property is that OBF models are linear in the coefficients  $\theta_i^\pm$  (cfr. Figure 1). The approximation of a RIR  $h(n)$  as a combination of exponentially decaying sinusoidal responses  $\varphi_i^\pm(n, \mathbf{p}_i)$  consists in estimating the pole parameters  $\mathbf{p}_i = \{p_i, p_i^*\}$  and the linear coefficients  $\boldsymbol{\theta}_i = \{\theta_i^+, \theta_i^-\}$  (where  $i = 1, \dots, m$ ) that minimize the distance between  $h(n)$  and the approximated response  $\hat{h}(n, \mathbf{p}, \boldsymbol{\theta})$  for  $n = 1, \dots, N$  (with  $n = t/f_s$  the discrete time variable). Given the sets  $\mathbf{p} = \{\mathbf{p}_1, \dots, \mathbf{p}_m\}$  and  $\boldsymbol{\theta} = \{\boldsymbol{\theta}_1, \dots, \boldsymbol{\theta}_m\}$ , the output  $\hat{h}(n, \mathbf{p}, \boldsymbol{\theta})$  of an OBF model for an impulse input signal  $\delta(n)$  is the linear combination of the  $2m$  basis functions  $\varphi_i^\pm(n, \mathbf{p}_i) = [N_i^\pm(z)P_i(z) \prod_{j=1}^{i-1} A_j(z)]\delta(n)$ ,

$$\hat{h}(n, \mathbf{p}, \boldsymbol{\theta}) = \sum_{i=1}^m \varphi_i^+(n, \mathbf{p}_i)\theta_i^+ + \sum_{i=1}^m \varphi_i^-(n, \mathbf{p}_i)\theta_i^- \quad (4)$$

or  $\hat{h}(n, \mathbf{p}, \boldsymbol{\theta}) = \boldsymbol{\varphi}(n, \mathbf{p})^T \boldsymbol{\theta}$ , where  $\boldsymbol{\varphi}(n, \mathbf{p})$  is a vector containing the impulse responses  $\varphi_i^\pm(n, \mathbf{p}_i)$  at time  $n$ . For a fixed set of poles  $\mathbf{p}$ , the problem of estimating the coefficients in  $\boldsymbol{\theta}$  becomes linear and can be solved in closed form using linear regression. By stacking all the vectors  $\boldsymbol{\varphi}(n, \mathbf{p})$  for  $n = 1, \dots, N$  in a matrix  $\boldsymbol{\Phi}(\mathbf{p})$ , the optimal values in the least-squares sense for a given data set  $\{\mathbf{h}\} = \{h(n)\}_{n=1}^N$  are obtained as  $\hat{\boldsymbol{\theta}} = \boldsymbol{\Phi}(\mathbf{p})^T \mathbf{h}$ , given that the orthonormality of the basis functions implies  $\boldsymbol{\Phi}(\mathbf{p})^T \boldsymbol{\Phi}(\mathbf{p}) = I_N$ .

The problem then reduces to the estimation of the poles, requiring in principle nonlinear estimation methods. The only known nonlinear method for the estimation of the poles for RIR approximation using OBF is the one proposed in [9]. In [11], the nonlinear problem was avoided by selecting poles from a large grid of candidate poles using a convex optimization method. An iterative greedy algorithm, called OBF-MP, was introduced in [10], which is scalable and numerically well-conditioned. In the following section, the OBF-MP algorithm is modified in order to jointly estimate a set of poles, common to multiple RIRs measured in the same room.

### 3. OBF-GMP algorithm

The OBF-MP [10] is a matching pursuit algorithm which at each iteration selects the predictors, i.e. the pair of basis functions, that are most correlated with the current residual part of the RIR. The candidate predictors are generated based on a grid  $\mathbf{p}_g =$

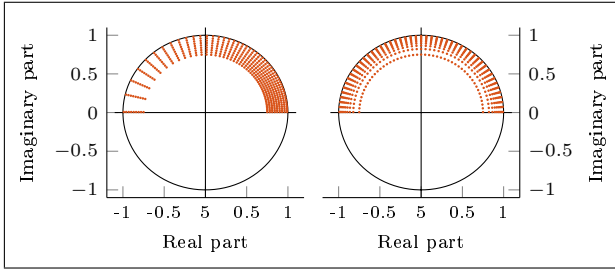


Figure 2. Pole grids using 500 poles, with 50 values for the angle  $[1, f_s/2-1]$  Hz and 10 values for the radius  $[0.75, 0.99]$ . (left) Logarithmic angles. (right) Logarithmic radii.

$\{p_1, \dots, p_G\}$  of poles distributed inside the unit circle. The distribution of the poles in the grid is arbitrary and can be dictated by the desire of a higher spectral resolution in the frequency range of interest or by other considerations based on prior knowledge about the acoustics of the room. Two examples are given in Figure 2. The left example shows a pole grid with angles distributed logarithmically, which yields a higher resolution at low frequencies. The right example shows a pole grid with radii distributed logarithmically, which yields a higher resolution close to the unit circle. At each iteration, the matrix  $\Phi_k(\mathbf{p}_g)$  is built with the basis functions computed for each pole in the grid  $\mathbf{p}_g$  and orthogonalized to the basis functions added in previous iterations. The OBF-MP algorithm is scalable. In fact, since the resulting filter structure is orthogonal by construction, the linear coefficients do not have to be recomputed at each iteration. As a consequence, the model order does not have to be determined beforehand and more poles can be added just by running extra iterations. At each iteration, the approximation error is reduced and the algorithm can be stopped when the desired degree of accuracy is obtained. Orthogonality also implies that the linear coefficients correspond to the correlation of the basis functions with the RIR. It follows that no matrix inversion operation is involved in the algorithm, avoiding any problem of numerical ill-conditioning.

Here, the OBF-MP algorithm is modified in order to estimate a set of poles which is common to a set of  $R$  RIRs measured in the same room. The modified algorithm, called OBF-GMP (Group Matching Pursuit), is intended to reduce the number of parameters necessary to represent the RIRs by identifying the resonant characteristics of the room, common to all RIRs. The OBF-GMP algorithm, listed below in details, works as follows. First, a grid  $\mathbf{p}_g$  of  $G$  candidate poles has to be defined. Then, the  $R$  target RIRs  $\mathbf{h}^r = \{h_r(n)\}_{n=1}^N$  are stacked in a matrix  $\mathbf{Y} = [\mathbf{h}^1, \dots, \mathbf{h}^R]$ , and the current residual matrix  $\mathbf{E}_0 = [\boldsymbol{\epsilon}_0^1, \dots, \boldsymbol{\epsilon}_0^R]$  is initialized as  $\mathbf{Y}$ . At each iteration  $k$ , OBF-GMP selects the pair of predictors in  $\Phi_k$  having maximum correlation with the residual signal vectors in  $\mathbf{E}_k$ . For a pair of complex-conjugate poles  $\{p_i, p_i^*\}$ , the correlation  $\alpha_i^r$  with each residual vector

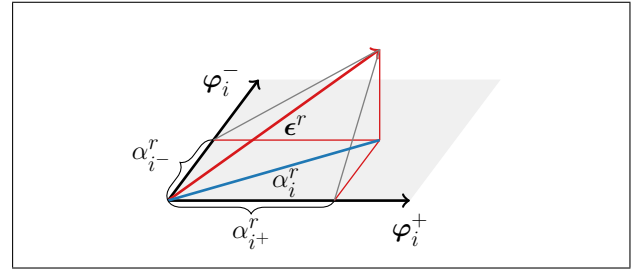


Figure 3. Graphical interpretation of the correlation between the residual vector  $\boldsymbol{\epsilon}$  and the predictors of a pair of complex-conjugate poles  $\{p_i, p_i^*\}$ .

---

#### Algorithm 1 OBF-GMP algorithm

---

- 1:  $\mathbf{p}_g = \{p_1, \dots, p_G\}$  ▷ Define poles in the pole grid
  - 2:  $n_A = 0, k = 0$  ▷  $n_A$ : # of selected predictors,  $k$ : iterations
  - 3:  $\mathbf{E}_0 = \mathbf{Y}, \hat{\mathbf{Y}}_0 = \mathbf{0}$ , ▷ Initialize signal vectors
  - 4: **while**  $n_A < M$  **do** ▷  $M$ : desired model order
  - 5:   Build  $\Phi_k(\mathbf{p}_g)$  ▷  $\Phi_k$ : matrix of candidate predictors  $\varphi_i$
  - 6:    $j = \arg \max_i \sum_{r=1}^R |\alpha_i^r|$  ▷ Max. correlation with  $\mathbf{E}_k$
  - 7:    $n_A = n_A + 2$  ▷ Update # of selected predictors
  - 8:    $\hat{\boldsymbol{\epsilon}}_k^r = [\varphi_j^+ \varphi_j^-][\alpha_j^+ \alpha_j^-]^T$  ▷ Update approx. residual
  - 9:    $\hat{\mathbf{E}}_k = [\hat{\boldsymbol{\epsilon}}_k^1, \dots, \hat{\boldsymbol{\epsilon}}_k^R]$  ▷ Current approx. residual matrix
  - 10:    $\hat{\mathbf{Y}}_{k+1} = \hat{\mathbf{Y}}_k + \hat{\mathbf{E}}_k$  ▷ Update target approx. matrix
  - 11:    $\mathbf{E}_{k+1} = \mathbf{E}_k - \hat{\mathbf{E}}_k$  ▷ Update current residual matrix
  - 12:    $k = k + 1$
  - 13: **end while**
- 

$\boldsymbol{\epsilon}_k^r$  is chosen as the projection of  $\boldsymbol{\epsilon}_k^r$  on the plane defined by predictors  $\varphi_i^+$  and  $\varphi_i^-$  (see Figure 3), and is given by

$$\alpha_i^r = \sqrt{\alpha_{i+}^{r2} + \alpha_{i-}^{r2}} = \sqrt{(\varphi_i^+ \boldsymbol{\epsilon}_k^r)^2 + (\varphi_i^- \boldsymbol{\epsilon}_k^r)^2}. \quad (5)$$

For each pair of complex-conjugate poles, the correlations with all the residual vectors in  $\mathbf{E}_k$  are then summed together, and the pole pair  $\{p_j, p_j^*\}$  selected is the one with index

$$j = \arg \max_i \sum_{r=1}^R |\alpha_i^r|. \quad (6)$$

Given the orthogonal construction of the basis functions, each approximated residual vector is obtained as  $\hat{\boldsymbol{\epsilon}}_k^r = [\varphi_j^+ \varphi_j^-][\alpha_j^+ \alpha_j^-]^T$  and stacked in the matrix  $\hat{\mathbf{E}}_k$ , which is used for updating the current target approximation matrix  $\hat{\mathbf{Y}}_k = \hat{\mathbf{E}}_k + \hat{\mathbf{Y}}_{k-1}$ , where  $\hat{\mathbf{Y}} = [\hat{\mathbf{h}}^1, \dots, \hat{\mathbf{h}}^R]$ , and the residual signal matrix  $\mathbf{E}_{k+1} = \mathbf{E}_k - \hat{\mathbf{E}}_k$ . The algorithm terminates when the desired number  $M$  of functions in the basis is reached or when the approximation error falls below a desired value.

Table I. Room specifications. Reverberation time calculated with the backward integration method [18].

Dimensions	6.35 L × 4.09 W × 2.40 H (m)
Reverberation Time	$T_{31.5\text{Hz}} = 1.44\text{s}$ $T_{40\text{Hz}} = 0.69\text{s}$ $T_{50\text{Hz}} = 0.74\text{s}$ $T_{63\text{Hz}} = 0.53\text{s}$ $T_{100\text{Hz}} = 0.47\text{s}$ $T_{125\text{Hz}} = 0.62\text{s}$



Figure 4. Sketch of the room at B&O headquarters, Struer, Denmark.

#### 4. RIR database

The RIR measurements used in the simulations were performed in an unoccupied, standard domestic listening room, sketched in Figure 4, based at Bang & Olufsen headquarters in Struer, Denmark. When furnished, the room complies with IEC 60268-13 [14] with  $RT_{(500\text{Hz}-1\text{kHz})} = 0.35\text{ s}$ . The room comprises of wooden floor, wooden false ceiling filled with Rockwool<sup>®</sup>, and lightly plastered painted walls with high-frequency absorbing panels on the side walls. During the measurements, the room was emptied, except for 8 acoustic wooden panels ( $0.5 \times 0.5 \times 0.025\text{ m}$ ) and 2 Helmholtz absorbers tuned at 200-300 Hz. The room dimensions and the values of the reverberation time are given in Table I. RIR measurements were obtained using the logarithmic sine-sweep technique [15] with a sampling rate of 48 kHz. The sweeps were recorded with a B&K 4939 1/4" microphone and B&K 2669 preamplifier, connected to an audio interface (RME UCX) and a laptop computer. Recordings of 3 s sine sweeps (0.1 Hz-1 kHz) produced by a custom Genelec 1094A subwoofer (12-150 Hz,  $\pm 3\text{ dB}$ ) were completed for 24 source-microphone positions (see Table II), in conformity with the guidelines in ISO 3382-1,2 [16, 17] for precision measurements. The RIR database measurements are available for download at <http://www.dreams-itn.eu/index.php/dissemination/downloads/subrir>.

#### 5. Simulation Results

The simulations results presented here aim at comparing the OBF-GMP algorithm with OBF-MP and the all-zero modeling. The obtained models are compared in terms of their ability to approximate a set of

Table II. Microphone and speaker positions. Speaker Position indicates the center of the transducer.

Mic	X	Y	Z	Src	X	Y	Z
1	1.12	1.56	1.50	1	3.84	3.84	0.53
2	0.77	4.04	1.80	2	2.90	0.80	0.53
3	2.04	4.47	0.90	3	3.63	5.83	0.53
4	1.62	5.32	0.60	4	2.35	4.55	1.13
5	3.05	3.06	1.50				
6	3.09	5.07	1.00				

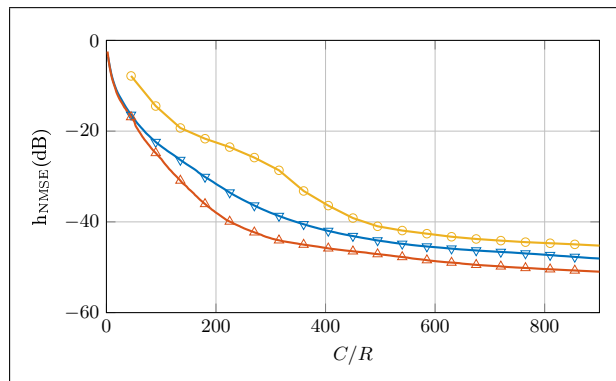


Figure 5. The average NMSE w.r.t. the number of model parameters  $C$  per RIR. The average NMSE in (7) for the entire time-response. All-Zero model ( $\circ$ ), OBF-GMP model ( $\triangle$ ), and OBF-MP model ( $\nabla$ ).

$R$  RIRs for a given number of parameters. For the all-zero modeling, the number of parameters is  $R$  times the number of taps used in the FIR filter for each response. For the OBF models (see Figure 1), the number of parameters is the number of poles  $m$  plus the number of linear coefficients  $2m$ , which sum up to  $3m$  coefficients. When estimating  $m$  poles individually for each RIR with OBF-MP, the total number of parameters is  $3mR$ . In case  $m$  poles are estimated jointly for all RIRs with OBF-GMP, only one common set of  $m$  poles is necessary, and the total number of parameters becomes  $m + 2mR$ .

The different models were tested on  $R = 22$  RIRs taken from the database introduced in Section 4. Each RIR was downsampled to  $f_s = 800\text{ Hz}$  and truncated to  $N = 4000$  samples from the first strong peak, selected as its starting point. The OBF-GMP pole grid used  $G = 1000$  poles with 20 different radii distributed logarithmically from 0.75 to 0.99 and with 50 different angles placed linearly in the range  $[1, f_s/2 - 1]\text{ Hz}$  (right plot of Figure 2). The error measure used to compare the performance of different models with the same number of parameters is the Normalized Mean-Square-Error (NMSE) in the time domain, averaged over all RIRs, given by

$$h_{\text{NMSE}} = 10 \log_{10} \frac{1}{R} \sum_{r=1}^R \frac{\|\mathbf{h}^r - \hat{\mathbf{h}}^r\|_2^2}{\|\mathbf{h}^r\|_2^2}. \quad (7)$$

Figure 5 shows the average NMSE produced by the OBF models using the two algorithms and by the all-

zero modeling, for the same total number of model parameters per RIR. It can be seen that the OBF models provide a better approximation compared to the all-zero model. Moreover, there is a significant reduction in the approximation error when OBF-GMP is used instead of OBF-MP, mainly resulting from the use of a larger number of poles (about 30% more). The fact that this improvement is not noticeable when the number of parameters is small can be explained by observing that OBF-MP tends to select poles closer to the unit circle, which approximate better the main strong resonances of the target magnitude response with a small number of poles.

## 6. Conclusions and Future Work

OBF models can be successfully used to approximate a RIR as a linear combination of exponentially decaying sinusoids, motivated by the physical definition of the RIR. In this paper, the OBF-MP algorithm proposed in [10] for the estimation of the poles, was modified in order to approximate multiple RIRs jointly. The idea is also exploited in the CAPZ model, with the difference that in the CAPZ model the estimation of the parameters is not scalable, thus requiring the order of the model to be determined in advance. Simulation results on a set of low-frequency RIRs measured in a rectangular room show that the OBF-GMP allows to reduce the number of parameters, obtaining a more compact representation of multiple RIRs.

Future research will further investigate the topic in the pursuit of a better understanding of the behavior of the OBF-GMP algorithm w.r.t. different numbers of RIRs or different configurations of the pole grid, also including a comparison with the CAPZ modeling. Moreover, the choice of the pole grid could be informed by prior knowledge about the characteristics of the room.

## Acknowledgement

This research work was carried out at the ESAT Laboratory of KU Leuven, in the frame of (i) the FP7-PEOPLE Marie Curie Initial Training Network 'Dereverberation and Reverberation of Audio, Music, and Speech (DREAMS)', funded by the European Commission under Grant Agreement no. 316969, (ii) KU Leuven Research Council CoE PFV/10/002 (OPTEC), (iii) the Interuniversity Attractive Poles Programme initiated by the Belgian Science Policy Office: IUAP P7/19 'Dynamical systems control and optimization' (DYSCO) 2012-2017, (iv) KU Leuven Impulsfonds IMP/14/037, (v) and was supported by a Postdoctoral Fellowship of the Research Foundation Flanders (FWO-Vlaanderen). The authors would like to thank Bang & Olufsen for the use of their premises and equipment. The scientific responsibility is assumed by its authors.

## References

- [1] J. Mourjopoulos and M. A. Paraskevas, "Pole and zero modeling of room transfer functions," *J. Sound Vib.*, vol. 146, no. 2, pp. 281–302, 1991.
- [2] G. Long, D. Shwed, and D. Falconer, "Study of a pole-zero adaptive echo canceller," *IEEE Trans. Circuits Syst.*, vol. 34, no. 7, pp. 765–769, 1987.
- [3] Y. Haneda, S. Makino, and Y. Kaneda, "Common acoustical pole and zero modeling of room transfer functions," *IEEE Trans. Speech Audio Process.*, vol. 2, no. 2, pp. 320–328, 1994.
- [4] P. Heuberger, P. van den Hof, and B. Wahlberg, *Modelling and Identification with Rational Orthogonal Basis Functions*. Springer, 2005.
- [5] P. S. C. Heuberger, P. M. J. Van den Hof, and O. Bosgra, "A generalized orthonormal basis for linear dynamical systems," *IEEE Trans. Autom. Control*, vol. 40, no. 3, pp. 451–465, 1995.
- [6] B. Ninness and F. Gustafsson, "A unifying construction of orthonormal bases for system identification," *IEEE Trans. Automatic Control*, vol. 42, no. 4, pp. 515–521, 1997.
- [7] H. Kuttruff, *Room acoustics*, 5th ed. Spon Press, 2009.
- [8] L. S. Ngia, "Recursive identification of acoustic echo systems using orthonormal basis functions," *IEEE Trans. Speech Audio Process.*, vol. 11, no. 3, pp. 278–293, 2003.
- [9] T. Paatero and M. Karjalainen, "Kautz filters and generalized frequency resolution: Theory and audio applications," *J. Audio Eng. Soc.*, vol. 51, no. 1/2, pp. 27–44, 2003.
- [10] G. Vairetti, T. van Waterschoot, M. Moonen, M. Catrysse, and S. H. Jensen, "An automatic model-building algorithm for sparse approximation of room impulse responses with orthonormal basis functions," in *IEEE Proc. IWAENC*, 2014.
- [11] —, "Sparse linear parametric modeling of room acoustics with orthonormal basis functions," in *Proc. EUSIPCO*, 2014.
- [12] B. Bank, "Perceptually motivated audio equalization using fixed-pole parallel second-order filters," *IEEE Signal Process. Lett.*, vol. 15, pp. 477–480, 2008.
- [13] P. W. Broome, "Discrete orthonormal sequences," *J. Assoc. Comput. Mach.*, vol. 12, no. 2, pp. 151–168, 1965.
- [14] IEC 60268-13:1998, "Sound system equipment - part 13: Listening tests on loudspeakers," 1998.
- [15] A. Farina, "Simultaneous measurement of impulse response and distortion with a swept-sine technique," in *Audio Eng. Soc. Conv. 108*, 2000.
- [16] ISO 3382-1:2009, "Acoustics - measurements of room acoustic parameters - part 1: Performance spaces," 2009.
- [17] ISO 3382-2:2008, "Acoustics - measurements of room acoustic parameters - part 2: Reverberation time in ordinary rooms," 2008.
- [18] M. R. Schroeder, "New method of measuring reverberation time," *J. Acous. Soc. Am.*, vol. 37, no. 3, pp. 409–412, 1965.